Rapid Communications
www.mrc-journal.de

Systematic Screening of Different Polyglycerin-Based Dienophile Macromonomers for Efficient Nanogel Formation through IEDDA Inverse Nanoprecipitation

*Alexander Oehrl, Sebastian Schötz, and Rainer Haag**

Alternatives for strain-promoted azide–alkyne cycloaddition (SPAAC) chemistries are needed because of the employment of expensive and not easily scalable precursors such as bicyclo[6.1.0]non-4-yne (BCN). Inverse electron demand Diels Alder (iEDDA)-based click chemistries, using dienophiles and tetrazines, offer a more bioorthogonal and faster toolbox, especially in the biomedical field. Here, the straightforward synthesis of dendritic polyglycerin dienophiles (dPG-dienophiles) and dPG-methyl-tetrazine (dPG-metTet) as macromonomers for a fast, stable, and scalable nanogel formation by inverse nanoprecipitation is reported. Nanogel size–influencing parameters are screened such as macromonomer concentration and water-to-acetone ratio are screened. dPG-norbonene and dPG-cyclopropene show fast and stable nanogel formation in the size range of 40–200 nm and are thus used for the coprecipitation of the model protein myoglobin. High encapsulation efficiencies of more than 70% at a 5 wt% feed ratio are obtained in both cases, showing the suitability of the mild gelation chemistry for the encapsulation of small proteins.

Therapeutic protein drugs are on the rise in the treatment of various diseases, due to their increased specificity compared to small molecules. However, they suffer the drawback of increased immune recognition and undergo renal clearance if their size is below the renal threshold of 45 kDa or a hydrodynamic diameter of about 5.5 nm.[1,2] In order to prevent the rapid clearance, the proteins are usually covalently modified with polyethylene glycol (PEG), also calles PEGylation, to increase their total molecular weight and reduce immune recognition.[3–6] However, PEG seems to be able to induce an immune response, as well as hypersensitivity reactions in some patients.[6]

Moreover, to prevent the immune recognition, therapeutic proteins can be masked by non-covalent encapsulation in nanocarriers such as nanogels.[7–10]

A. Oehrl, S. Schötz, Prof. R. Haag
Institute for Chemistry and Biochemistry
Department of Biology, Chemistry, and Pharmacy
Freie Universität Berlin
Takustr 3 D-14195, Berlin, Germany
E-mail: haag@chemie.fu-berlin.de

The ORCID identification number(s) for the author(s) of this article can be found under https://doi.org/10.1002/marc.201900510.

DOI: 10.1002/marc.201900510

These nanogels are commonly highly water-swollen polymer networks in the size range of 10–1000 nm that offer a stealth effect to any protein cargo inside, due to their hydrophilic nature and small and unspecific interactions with blood proteins.[10–14] The size of a nanogel is typically above the renal threshold, yielding increased circulation times for the encapsulated proteins. Furthermore, nanogels only physically entrap the protein instead of forming covalent bonds such as in the case of PEGylation, preventing any detrimental influence of covalent modifications.[3,6]

A variety of different methods are available for the preparation of nanogels. The most common preparation methods are the mini- and microemulsion polymerizations of monomers or macromonomers.[15–23] These methods utilize droplets of reactive monomers in the desired size range which are obtained by high energy input from ultrasonication in miniemulsion and large surfactant amounts in microemulsions. Subsequent crosslinking of the monomers in those templated droplets led to a dispersion of polymer beads in the nanometer to micrometer range. However, the use of ultrasonication and surfactants has the downside of not providing mild conditions for the in situ encapsulation of proteins and poses problems with purification.[23–25]

A very useful method for the preparation of hydrophobic nanoparticles is the nanoprecipitation method, which is based on the insolubility of certain growing polymers in a corresponding non-solvent.[26] For example, polystyrene (PS),[27] polylactic acid, and copolymers of polylactic and glycolic acid (PLA/PLA-co-PGA)[26,28] nanoparticles have been prepared in such a fashion. These polymers can be used for the encapsulation of hydrophobic drugs. Our group reported the use of an inverse nanoprecipitation method with hydrophilic macromonomers based on dendritic polyglycerol (dPG).[7] Due to the reversal of polarity in this method, a surfactant-free, mild, and easy to purify way of producing nanogels is offered. Proteins were encapsulated with high efficiency and retained their functionality upon release.

During inverse nanoprecipitation, the macromonomers form nanoaggregates due to the diffusion of the solvent into the non-solvent. These aggregates then must be crosslinked in order to obtain a stable polymer network that does not break up upon dilution with water. The type of crosslinking chemistry has thus a very big impact on the gel formation process. Click-type

reactions are especially suitable for this application. They are fast and usually proceed in a quantitative fashion.[29] Copper-catalyzed Huisgen 2 + 3 cycloaddition, for example, is based on the reaction of organic azides with terminal organic alkynes and has been used for the preparation of nanoparticles and nanogels.[29] The reactive groups are easily obtained, although the need of copper as a catalyst is a major drawback. Copper ions are usually hard to remove and can bind to some proteins and therefore subject cells to oxidative stress due to the production of reactive oxygen species, diminishing the biocompatibility of nanogels produced in such a manner.[30] Copper-free alternatives exist, where the terminal alkyne is replaced by a strained version, usually embedded in an eight-membered ring system.[31] These highly strained systems allow for the complete elimination of copper, because the ring-strain release upon reaction with the azide provides the driving force for the coupling reaction. Yet, some major drawbacks of these strain-promoted azide–alkyne cycloaddition (SPAAC) reactions are the high price for the precursor molecules, as well as the tedious and low-yielding synthetic protocols, especially for bicyclo[6.1.0]non-4-yne (BCN).

Another common crosslinking method, the thiol-ene reaction, is based on free thiols reacting with olefin derivatives. This method has the advantage of easily accessible macromonomers, which makes the process scalable and comparatively inexpensive. However, it is incompatible with proteins that contain free thiols.[32]

We have previously reported on nanogels, which are based on a hydrophilic, biocompatible, and easy to functionalize dPG-backbone.[33,34] A lot of the aforementioned different linking strategies have been used, such as CuAAC,[7] thiol-ene,[35,36] and the SPAAC reaction.[37]

Due to the drawbacks of some of these methods, the need for newer generations of click reactions arose. One of the most recent advances in "click chemistry" was the development of inverse electron demand Diels-Alder (iEDDA) reactions based on tetrazine derivatives and different dienophiles.[38–41] Depending on the dienophiles and tetrazines used, the reaction kinetics can be orders of magnitude faster than the corresponding SPAAC alternatives.[41]

IEDDA has been used as a bioorthogonal linking strategy for fluorescent labeling of antibodies,[42] DNA-tagging,[43] and even cell labeling.[44] Due to the fast reaction rates, iEDDA is considered more bioorthogonal than SPAAC, as any possible side reactions with biological systems are much slower.[45] There is a big variety of synthetically accessible tetrazine[46] derivatives and dienophiles. They all offer different reactivities and synthetic accessibility as well as stability in aqueous solutions.[46] Depending on the application, one can choose the most suitable combination of tetrazine and dienophile.

We hypothesize that these characteristics of iEDDA reactions are thus optimal for the substitution of SPAAC in the formation of nanogels by inverse nanoprecipitation.

We present the synthesis of new dPG-based macromonomers functionalized with methyl-tetrazine and different dienophiles such as the well-known norbonene, methylcyclopropene, and dihydropyran (DHP). The macromonomers are characterized by nuclear magnetic resonane (NMR) and dynamic light scattering (DLS) and tested regarding their ability to form macrogels, as well as stable nanogels during inverse nanoprecipitation in acetone. The most promising macromonomers dPG-norbonene and dPG-cyclopropene are used for the in situ coprecipitation of the small protein myoglobin (17 kDa) and show very good encapsulation efficiencies up to 93%. The fast and efficient synthetic route to dPG-norbonene and dPG-metTet, as well as the stable and scalable nanogels that are obtained from them, while avoiding the drawbacks of other crosslinking strategies makes this a possible new platform for the bioorthogonal encapsulation of therapeutic proteins.

The success of a nanocarrier depends on its key physical properties, such as the nature of the material that it is made of (e.g., functional groups), hydrophilicity/hydrophobicity balance, and the size, as well as the synthetic accessibility of the respective crosslinkers. We chose, for the purpose of a high biocompatibility and ease of functionalization, the already well known dPG.[33,34,47,48] Due to its large amount of terminal hydroxyl groups, it is highly hydrophilic and easy to functionalize without losing its hydrophilicity upon a low degree of functionalization. The polymer itself can be synthesized in kilogram scale which makes it a very suitable candidate as a macromonomer for nanogel synthesis.

We chose the inverse nanoprecipitation method for the formation of the nanogel network as no surfactant is needed and thus a mild encapsulation of proteins becomes possible. In order to achieve a stable gel in a fast way, the iEDDA chemistry was chosen as a gel crosslinking strategy due to its biorthogonality and high reaction rates. However, the stability of the reactive groups to reaction conditions, as well as storage conditions is also very important for potential applications.

For our work, we therefore selected a water stable tetrazine derivative, which still has a moderate reactivity toward dienophiles and can be easily attached to the dPG-core. 4-(6-Methyl-1,2,4,5-tetrazin-3-yl)benzoic acid was thus chosen, which can be attached via simple amide bond formation to a dPG-amine core. As the counterpart, four different dienophiles were chosen, in order to compare their reactivity during gel formation and the stability of the final nanogels in terms of aggregation. As can be seen in **Scheme 1**, we obtained four different dPG-dienophiles with approximately the same degree of functionalization starting from a 6 kDa dPG core. The different dPG-macromonomers are depicted as the corresponding colored spheres.

The synthetic overview for the precursor molecules **(1–5)** can be found in Scheme S1, Supporting Information.

One great advantage of using iEDDA chemistry compared to strained alkyne–azide cycloaddition is the accessibility of the reactive tetrazines and dienophiles. The tetrazine precursor 4-(6-methyl-1,2,4,5-tetrazin-3-yl)benzoic acid was obtained according to a one-pot reaction reported in literature in a moderate yield of 40% but can be used for functionalization with any kind of amine and has a good stability in water and buffer.[46] The different dienophiles were synthesized as the reactive carbonate derivatives. In this form, they can be reacted with any kind of amine, yielding the corresponding carbamate-linked dienophiles. In contrast, the synthesis of BCN is quite lengthy, with five steps and an overall yield of only 27%. In the series of dienophiles reported here, BCN is known to be one of the most reactive dienophiles in tetrazine click-reactions.[49] The next one in line in terms of reactivity is the cyclopropene derivative, which we obtained in four steps with a low overall

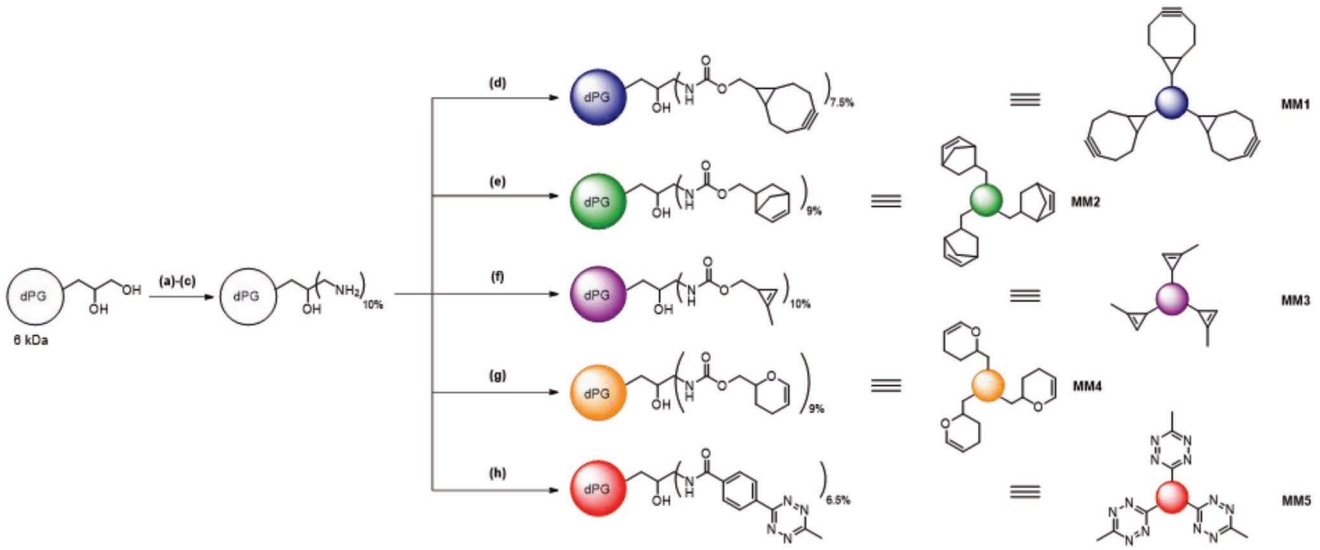

Scheme 1. Synthetic overview for the different macromonomers dPG-BCN, dPG-norbonene, dPG-cyclopropene, dPG-DHP, and dPG-metTet. The following conditions were used: a) MsCl, NEt_3, DMF, rt, overnight; b) NaN_3, 60 °C, 3 d; c) PPh_3, water/THF, rt, 3 d; d) 1, NEt_3, DMF, rt, overnight; e) 2, NEt_3, DMF, rt, overnight; f) 3, NEt_3, DMF, rt, overnight; g) 4, NEt_3, DMF, rt, overnight; and h) 5, HATU, DIPEA, DMF, rt, overnight. Number of reactive groups not representative; provided only for clarity.

yield of 19%. We chose the structural motive of bicyclo[2.2.1]hept-5-ene-2-carbaldehyde as a precursor as it is commercially available at a low price and was easily transformed in two steps with a good overall yield of 84% to the reactive carbonate form bicyclo[2.2.1]hept-5-en-2-ylmethyl (4-nitrophenyl) carbonate. Thus, norbonene was the most promising and well-known dienophile candidate in terms of potential upscaling and commercial use, even though it presents a relatively moderate reactivity.[50] The last dienophile we tested, was based on a common protecting group for alcohols. The (3,4-dihydro-2H-pyran-2-yl) methanol is commercially available for a relatively low price and is structurally related to DHP. The commercial precursor was transformed to the activated DHP carbonate (3,4-dihydro-2H-pyran-2-yl)methyl (4-nitrophenyl) carbonate in one step, with a yield of 79%. This structural motif is known as a dienophile in literature; although, the reaction rates are considerably lower compared to the other structural motives used in this work.[51]

With the reactive dienophiles and tetrazine in hand, the functionalization of the polymer core, dPG-amine, was performed in a straightforward fashion using the same procedure for every dienophile (Scheme 1). This provided us with a toolbox of macromonomers for the formation of nanogels. The macromonomers were characterized by NMR, IR, and DLS, as can be seen in the Supporting Information.

In a first screening, we used the macromonomers in the formation of macroscopic hydrogels to determine the reactivity of each type of dienophile. This was investigated by measuring the time required for the gelation of a mixture of dPG-metTet with the respective dPG-dienophile. As can be seen in **Figure 1**, the dPG-cyclopropene was the macromonomer with the fastest gelation time. It was followed in reactivity by dPG-norbonene. dPG-BCN and dPG-DHP did not show any macrogel formation even after 30 min.

Only an increased viscosity was observed for dPG-BCN. As BCN was supposed to have the highest reaction rates, we expected it to have the fastest macrogel formation. We hypothesized that, due to the fast reaction, the dPG-BCN was quenched almost instantaneously before a network formation could happen. The lower reactivity of cyclopropene and norbonene led to diffusion of macromonomers within the network and thus to a stable gel formation. As expected, the cyclopropene derivative reacted faster than the norbonene derivative. However, both showed macrogel formation in a reliable manner. Only dPG-DHP was too unreactive and did not yield even an increased viscosity of the macromonomer mix.

Subsequently, we performed the synthesis of nanogels via inverse nanoprecipitation. The process works by fast injection of a dilute macromonomer solution into the corresponding non-solvent. In our case, the non-solvent for dPG-based

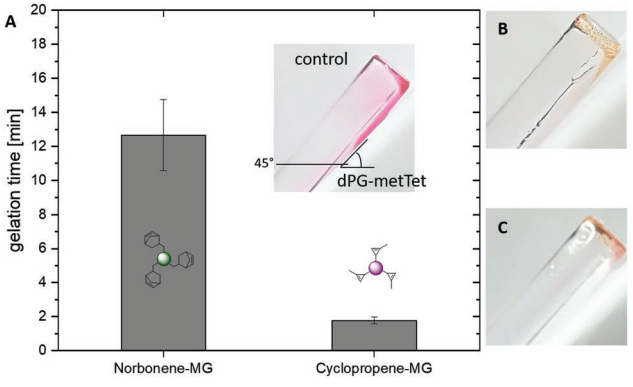

Figure 1. Macrogelation for the dPG-dienophiles MM2 and MM3, n = 3. A) Gelation times of MM2 and MM3 measured in triplicate. Control depicts the measurement setup with a small glass vial at an angle of 45° and MM5 without crosslinker. B) Macrogel of MM2 after 30 min. C) Macrogel of MM3 after 30 min.

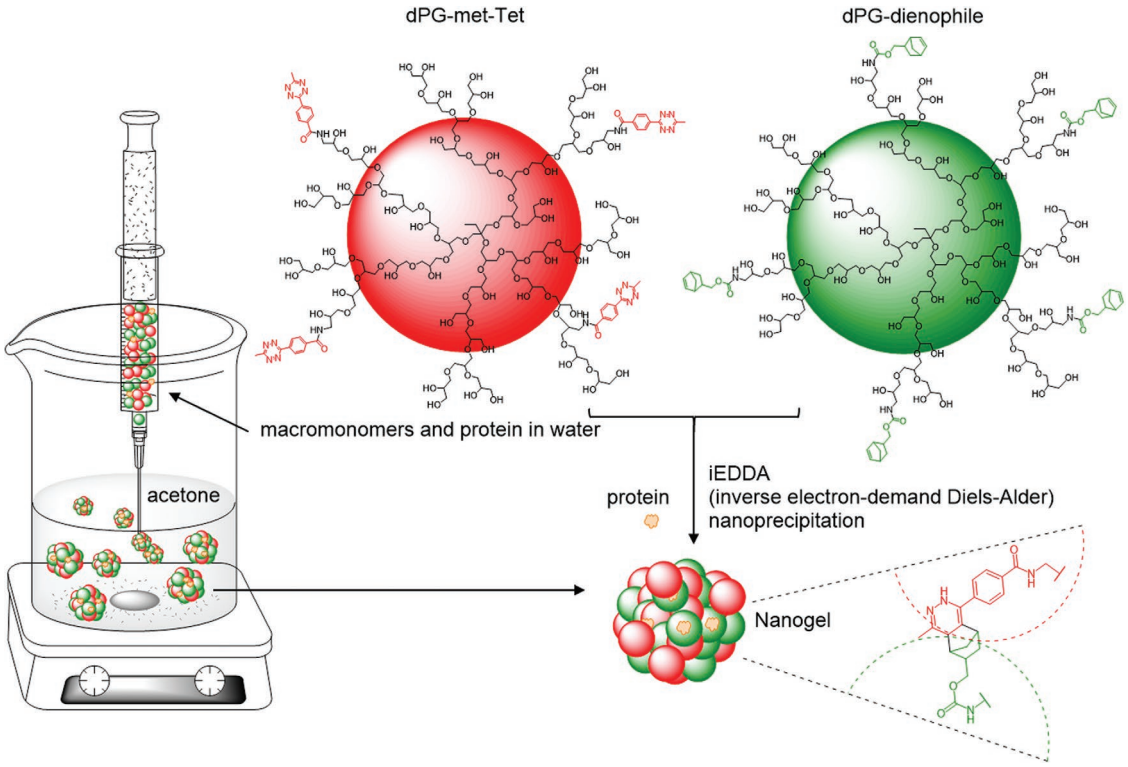

Scheme 2. Overview on nanogel formation by inverse nanoprecipitation in acetone with dPG-norbonene as an example. Linking points and structure of dPG-polymer core are shown. Possible encapsulation of myoglobin is shown.

polymers was acetone. The schematic overview on the inverse nanoprecipitation process can be seen in **Scheme 2**.

A lot of parameters can influence the outcome of the nanoprecipitation method such as macromonomer concentration, solvent/non-solvent ratio, stirring speed, temperature, macromonomer ratio, and reaction time. Usually, the size distribution and polydispersity are influenced by the parameters described above. For biomedical applications, nanogel sizes in the range of 20–200 nm are desirable.[52,53] We investigated most of these parameters for the most promising dienophile dPG-norbonene. The gels were produced by separately dissolving the respective macromonomers in water and then mixing dPG-dienophile with dPG-metTet, just prior to injection into acetone. Depending on the experiment, different amounts of the stock solutions were employed. The macromonomer solutions were cooled to 4 °C in order to prevent premature crosslinking.

First, the influence of the macromonomer concentration in water on the nanogel formation was studied. As can be seen in **Table 1**, the concentration was changed between 0.5 and 5 mg mL^{-1}.

The macromonomer concentration apparently did not have a relevant influence on the size or the polydispersity of the nanogels. However, for a concentration of 1 mg mL^{-1}, we observed a disturbed gel formation, that led to very large gels with a high polydispersity. As the macromonomer concentration in water directly correlates with the scalability of the process, we chose the highest concentration of 5 mg mL^{-1} for further studies.

In order to prevent subsequent crosslinking of already formed nanogels, an excess of one of the macromonomers was used. The ratio of reactive groups was set to 1:1.5. dPG-metTet exhibits a pink color, which can be used as an indicator of the status of the reaction. For this reason, dPG-metTet was used in shortfall to the other macromonomer to observe completion

Table 1. Concentration dependence of dPG-norbonene/dPG-metTet-NGs.

Entry	Macromonomer		V(H_2O): V(acetone)	$T_{q,\,chem}$ [min]	$T_{q,\,water}$ [min]	Z-average [nm]	PDI
	Ratio (A:B)	C [mg mL^{-1}]					
1	1:1.5	5	1:40	5	30	163 ± 13	0.02 ± 0.01
2	1:1.5	2.5	1:40	5	30	209 ± 21	0.03 ± 0.02
3	1:1.5	1	1:40	5	30	1528 ± 801	0.6 ± 0.1
4	1:1.5	0.5	1:40	5	30	190 ± 20	0.03 ± 0.02

A, dPG-metTet; B, dPG-norbonene; size values correspond to the mean of three individual gels.

Table 2. Dependence of water quenching time on dPG-norbonene/dPG-metTet-NGs.

Entry	Macromonomer		$T_{q,\ water}$ [min]	Z-average [nm]	PDI
	Ratio (A:B)	C [mg mL^{-1}]			
1	1:1.5	5	on	nd	nd
2	1:1.5	5	60	194 ± 6	0.07 ± 0.02
3	1:1.5	5	30	188 ± 9	0.07 ± 0.02
4	1:1.5	5	10	136 ± 5	0.07 ± 0.01
5	1:1.5	5	5	121 ± 4	0.06 ± 0.02
6	1:1.5	5	2.5	41 ± 4	0.40 ± 0.03
7	1:1.5	5	1	nd	nd

A, dPG-metTet; B, dPG-norbonene; nd, measurement quality criteria not achieved due to very high polydispersity; V(H_2O):V(acetone) = 1:40; $T_{q,\ chem}$ = 10 min; on = overnight.

of the reaction. Additionally, a chemical quencher (2-(vinyloxy)ethan-1-ol) was used in order to deactivate the remaining methyl-tetrazine groups. The influence of the time, after which the chemical quencher was added, on the nanogel formation is reported in Table S2 and Figure S2, Supporting Information.

No clear trend could be seen, as the size was in the same range for all different time points and the polydispersity index (PDI) stayed below 0.1. Apparently, the reaction rates were so fast for the crosslinking reaction that the chemical quencher did not have an influence on the nanogel formation, whatsoever. Aggregation of already formed nanogels was also not an issue, as even without the addition of a chemical quencher, the gels stayed stable and maintained their size (Table S2, Supporting Information, entry 1). In order to assure that no crosslinking would happen, we chose to add the chemical quencher anyway and used 10 min as the delay time for its addition.

Due to the stability of the system, which gave in most of the cases, reproducibly nanogels in the size range of 180–200 nm, we wanted to see if it is possible to influence the particle size while still maintaining a good PDI. As the crosslinking seemed to be almost complete after 10 min, we tried to physically quench the nanogel formation after defined time spans. Water was added to decrease the local macromonomer concentration and to break up any preformed aggregates that did not crosslink yet. As can be seen in **Table 2** and **Figure 2**, the nanogel size was not really affected after roughly 30 min. If the gels were not quenched at all, then complete precipitation occurred overnight (Table 2, entry 1). For quenching times of 60 and 30 min, there was no difference in nanogel size. However, quenching after 10 and 5 min showed a significant reduction in nanogel size while still maintaining a low PDI value of less than 0.1. Quenching at 1 and 2.5 min nanogel formation was severely hampered. Only small aggregates of around 40 nm were observed in DLS (vol%) for a reaction time of 2.5 min, whereas no reliable measurement could be obtained for a reaction time of 1 min. This trend of smaller particles after short reaction times can be explained with the dissolution of non-crosslinked aggregates. **Figure 3** shows the overall trend between water quenching time and nanogel size.

Due to the fast reaction rates the size distribution quickly reached saturation. Therefore, there is only a small time window to influence the size of the nanogels towards smaller values.

Another way to control the size of nanogels is to change the ratio of solvent to non-solvent. The right ratio depends on the actual solubility of the macromonomers in each solvent. For extremely high ratios of solvent to non-solvent, there will not be nanogel formation anymore as the macromonomers do not aggregate in very low amounts of the non-solvent. As the ratio decreases, the macromonomers can aggregate due to their decreasing solubility in the mixture of solvent and non-solvent.

The effect of several ratios of solvent and non-solvent, ranging from 1:20 to 1:200, are reported in **Table 3**.

For low ratios such as 1:200 to 1:80, the nanogel formation was strongly disturbed, leading to precipitation. Meaningful size values could not be determined, because the measurement quality was not achieved in DLS. Ratios of 1:60 to 1:20, however, were suitable for nanogel formation, with higher ratios leading to smaller nanogels. The polydispersity of the gels was in all cases below 0.1, which suggested a stable gel formation for such high ratios of solvent to non-solvent. This was a very promising result, as the main drawback of the inverse nanoprecipitation method is that very high amounts of non-solvent are needed for the preparation of relatively small amounts of

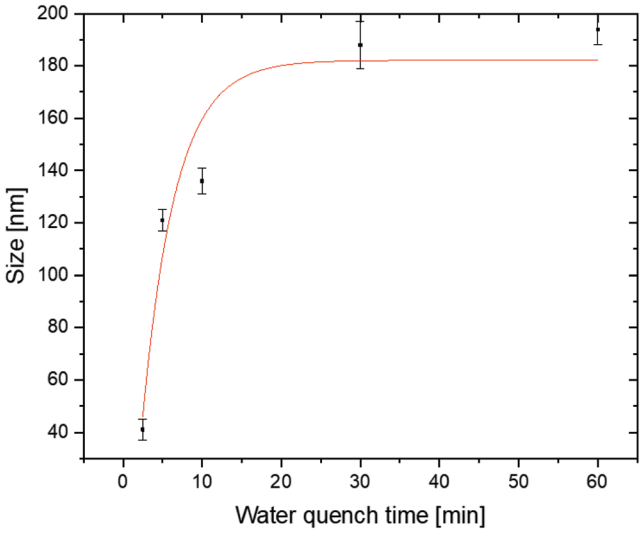

Figure 2. Dependency of nanogel size on water quenching time.

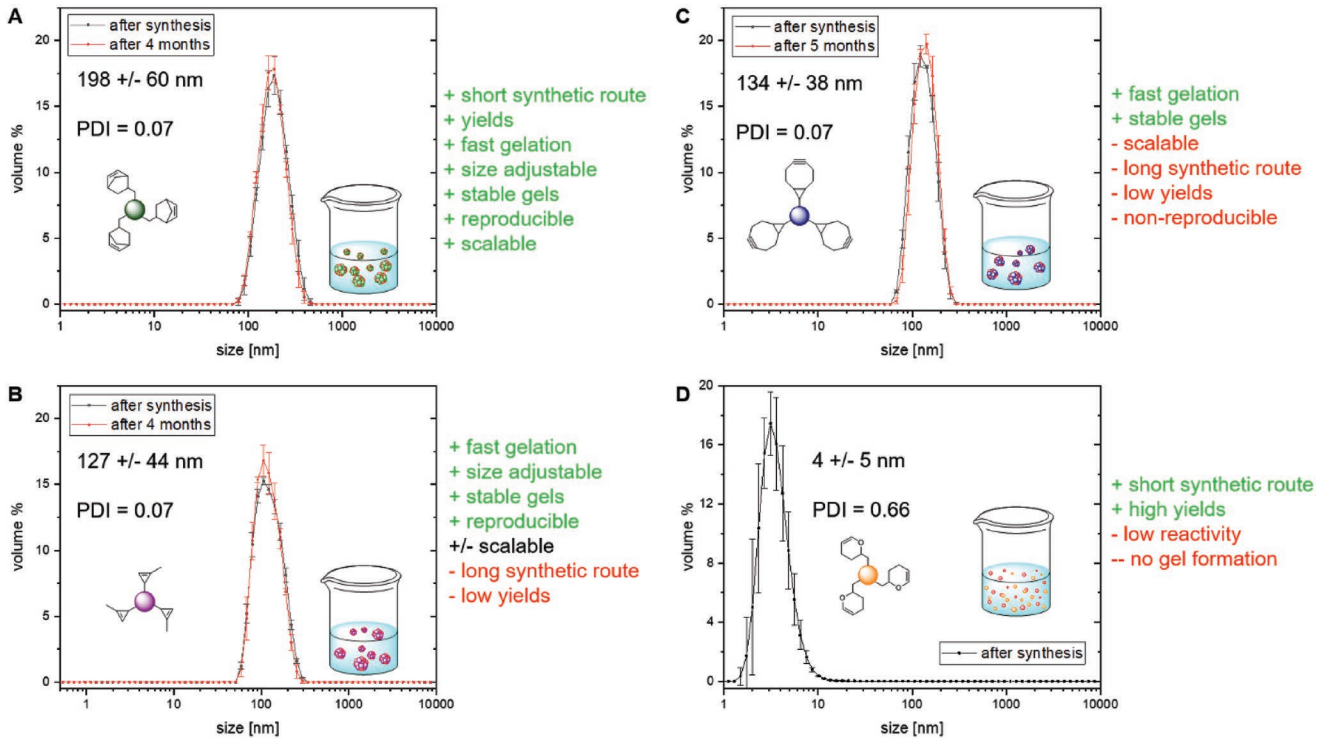

Figure 3. Overview on nanogel formation behavior, synthetic accessibility, and reactivity of the different macromonomers. DLS measurement of an exemplary gel is shown for each macromonomer, directly after synthesis and purification (black line) and after 4 to 5 months (red line). A) dPG-norbonene NG, B) dPG-cyclopropene NG, C) dPG-BCN NG, and D) dPG-DHP + dPG-metTet.

nanogels, usually a ratio of 1:200. Obtaining stable and almost monodisperse nanogels with a relatively high ratio of 1:20 means that the nanogel formation is scalable. For all batches, we used 5 mg of macromonomers, as higher amounts make it usually time consuming to remove acetone. To obtain relevant amounts of nanogels, we wanted to confirm if the production process is scalable to ten times the amount that is usually taken for a gel batch. **Table 4** shows the obtained nanogels for 50 mg batches.

Gels in the size range of 100–120 nm were obtained with PDI values below 0.1. The three gels were combined to yield a single dispersion of nanogel in water, with an average size distribution between the three gels and a PDI value of 0.1. This showed that several batches could be combined without a big increase in polydispersity. The scalability of a single batch and the possible combination of several batches into one batch thus holds the possibility to produce these nanogels in gram scale.

The stirring speed can also influence the nanogel formation. Table S3 and Figure S3, Supporting Information show the effect of different stirring speeds on the size and polydispersity of the nanogels. The stirring speed had no relevant influence on the size and PDI of the nanogels, although the same volume of non-solvent was used for each stirring speed. Thus, the highest stirring speeds were used for all the experiments.

The other combinations of macromonomers were then studied. Starting with the lowest reactivity, dPG-DHP was

Table 3. dPG-norbonene/dPG-metTet-NGs; water:acetone ratios.

Entry	Macromonomer		$V(H_2O)$: V(acetone)	Z-average [nm]	PDI
	Ratio (A:B)	C [mg mL^{-1}]			
1	1:1.5	5	1:200	nd	nd
2	1:1.5	5	1:150	nd	nd
3	1:1.5	5	1:100	nd	nd
4	1:1.5	5	1:80	nd	nd
5	1:1.5	5	1:60	233 ± 10	0.06 ± 0.01
6	1:1.5	5	1:40	165 ± 7	0.06 ± 0.01
7	1:1.5	5	1:20	110 ± 4	0.09 ± 0.01

A, dPG-metTet; B, dPG-norbonene; nd, measurement quality criteria not achieved due to very high polydispersity; $T_{q,\,chem}$ = 10 min and $T_{q,\,water}$ = 30 min.

Table 4. Nanogel formation of dPG-norbonene/dPG-metTet (50 mg batch size).

Entry	Macromonomer		Z-average [nm]	PDI
	Ratio (A:B)	C [mg mL^{-1}]		
1	1:1.5	5	122 ± 1	0.07 ± 0.01
2	1:1.5	5	129 ± 2	0.07 ± 0.01
3	1:1.5	5	104 ± 2	0.07 ± 0.01
Avg.	1:1.5	5	118 ± 11	0.07 ± 0.01

A, dPG-metTet; B, dPG-norbonene; V(H_2O):V(acetone) = 1:40; $T_{q,\,chem}$ = 5 min; and $T_{q,\,water}$ = 30 min.

tested regarding its ability to form nanogels. As already shown, the macrogel experiments did not yield any gel after extended periods of time for dPG-DHP. Even after a reaction time of 18 h, only the non-crosslinked macromonomers could be seen by DLS (Figure 3). This showed that the reactivity of the DHP moiety was far too low for a nanogel formation. Thus, we decided to not investigate the dPG-DHP macromonomer further as useful time spans for gel formation could not be achieved.

dPG-BCN showed a delayed and incomplete gelation during macrogel formation. As can be seen in Tables S4 and S5, Supporting Information, the optimal conditions for nanogel formation, which were observed for dPG-norbonene, were also tested for dPG-BCN. The nanogel formation leads almost in all cases to big aggregates with high polydispersities, which are also not dependent on the preparation conditions. No reproducibility could be observed under the tested conditions, as size values scattered from 100 to 2000 nm, with PDI values between 0.2 and 0.8. We assumed that the high reactivity of BCN led to premature crosslinking and further crosslinking of the nanoaggregates that formed during the inverse nanoprecipitation. This resulted in a very fast growth of bigger and bigger aggregates. This might explain the big and polydisperse gels we observed with this macromonomer.

The last macromonomer that was tested was dPG-cyclopropene. The cyclopropene moiety is rather small compared to the alternatives presented in this work and in literature. In general, it does not have as big of an influence on hydrophilicity as dienophiles, such as BCN. Moreover, the reactivity toward tetrazine derivatives is also reported to be moderately high.[54] However, the synthesis reported in literature is quite lengthy. Hence, it could be an alternative to norbonene, in cases where very small and less hydrophobic crosslinkers are needed, despite the drawback of low scalability. As for the other macromonomers, different conditions were tested, which are summarized in Table S6, Supporting Information. dPG-cyclopropene, as well as dPG-norbonene, showed stable nanogel formation in the size range of 70–120 nm. This macromonomer also yielded nanogels with very low polydispersity indices of below 0.1.

Zeta potential measurements (Figure S4, Supporting Information) showed that all gels had a close to neutral surface charge. dPG-norbonene and dPG-cyclopropene nanogels were slightly positively charged and dPG-BCN nanogels slightly negatively charged.

A summary of the nanogel formation process for the different macromonomers is described in Figure 3 and the corresponding NTA measurements can be found in Figure S5, Supporting Information.

Of all the dienophiles, dPG-norbonene and dPG-cyclopropene showed reliably nanogel formation in the biologically relevant size range of below 100–200 nm. The most influencing parameters on nanogel size and polydispersity were water to acetone ratio and the water quenching time $T_{q,water}$. dPG-norbonene, however, is by far the most promising candidate for the easy upscaling and robust application, due to the straightforward synthesis of the precursors and the stable and monodisperse nanogels which can be obtained.

Due to their stable and reproducible nanogel formation, dPG-norbonene and dPG-cyclopropene were used in coprecipitation experiments with the protein myoglobin. During the mild coprecipitation, the protein was first physically encapsulated by the formation of nanoaggregates in the acetone phase. This polyglycerol shell around the protein protects it from the organic solvent and provides, due to the many hydroxyl groups, an almost natural environment to it. As the aggregates of polyglycerol macromonomers start to crosslink, the protein stays physically entrapped in the growing polymer network and diffusion gets ever more hindered. Due to the very mild reaction conditions of iEDDA and the absence of surfactants, high temperature and radicals, the sensitive protein cargo is very likely to be intact after nanogel formation.

Myoglobin, a small 17 kDa protein which is mostly responsible for oxygen transport within muscle tissue, was used as an inexpensive and abundant model protein for coprecipitation. We tested two different myoglobin feed ratios, a higher 5 wt% and lower 2.5 wt% of myoglobin compared to macromonomer. Tables S7 and S8, Supporting Information summarize the conditions we used and the nanogel sizes and polydispersity values that were obtained for dPG-norbonene and dPG-cyclopropene macromonomers, respectively.

The addition of a protein to the system changes the aggregation behavior during inverse nanoprecipitation significantly. The sizes of the nanogels at least doubled compared to the same conditions without protein (**Figure 4**A). However, the polydispersity indices of the formed nanogels, stayed low (below 0.1).

The determination of protein concentration within the gels was performed by a bicinchoninic acid (BCA) assay using bovine serum albumin (BSA) and myoglobin standard curves (Figures S6 and S7, Supporting Information). The total amount of protein was determined by multiplying the concentration of protein, determined in the BCA assay, by the total volume

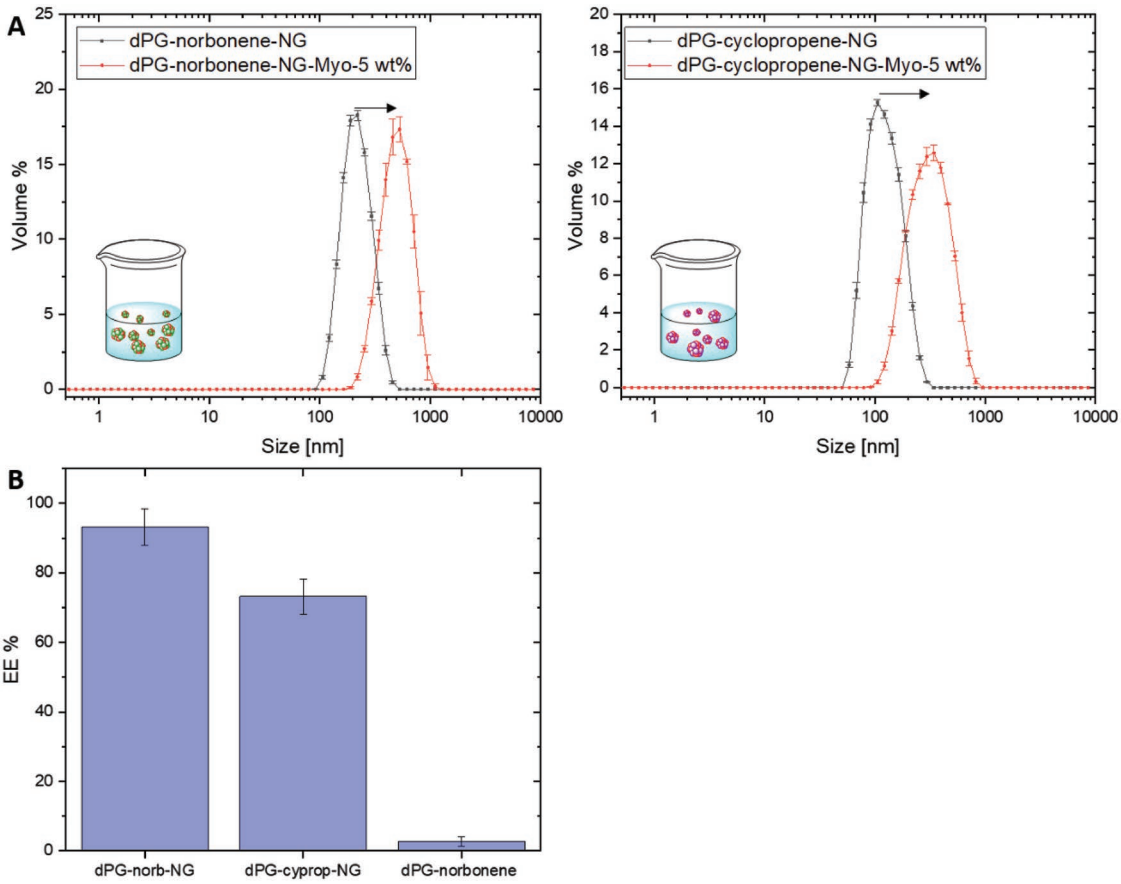

Figure 4. Influence of coprecipitation of myoglobin on nanogel size for dPG-norbonene and dPG-cyclopropene nanogels at 5 wt% myoglobin feed. A) left: DLS data for a dPG-norbonene-NG without (black line) and with (red line) encapsulated myoglobin; right: DLS data for dPG-cyclopropene-NG without (black line) and with (red line) encapsulated myoglobin. B) Encapsulation efficiency at 5 wt% feed of myoglobin in dPG-norbonene and dPG-cyclopropene nanogels. dPG-norbonene without dPG-tetrazine was used as a control, $n = 3$.

of the individual gel dispersions and then divided by the feed amount of protein. The results can be seen in Figure 4.

Both dPG-norbonene as well as dPG-cyclopropene nanogels could encapsulate myoglobin with a very high encapsulation efficiency of 75–93% at 5 wt% feed. The control shows only dPG-norbonene without dPG-metTet as crosslinker. The control sample was treated in the same way as the other samples, however, as no crosslinker was present, no gel formation was expected. Thus, no protein should have been present after centrifugal filtration. As confirmation, almost no protein was observed in the control experiments.

The results clearly showed, that the nanogels, which were formed through iEDDA click chemistry, especially the dPG-norbonene-based NGs, could efficiently encapsulate myoglobin.

We have shown the synthesis of different amine-reactive dienophiles as a toolbox for the functionalization of dPG-amine. The activated carbonates of norbonene, BCN, cyclopropene, and DHP were synthesized. The corresponding carbamate-linked dPG-dienophiles were obtained by a standardized procedure. The macromonomers dPG-norbonene and dPG-cyclopropene showed a fast macrogel formation within 12 min and nanogels in the size range of 40–200 nm were obtained with excellent polydispersity indices of 0.1 and below. dPG-norbonene-based nanogels were reproducibly synthesized under a wide range of conditions and showed batch scalability to at least 50 mg per batch. Combination of different batches yielded gels that retained the low polydispersity of the individual batches. dPG-BCN and dPG-DHP showed non-reproducible or no gel formation at all, respectively. In case of dPG-BCN, the reason was probably due to very high reaction rates and thus premature cross-linking and, in the case of dPG-DHP, a very low reactivity and hence, no crosslinking at all.

Coprecipitation of myoglobin (17 kDa) showed excellent encapsulation efficiencies of up to 93% for nanogels made from dPG-norbonene and dPG-cyclopropene, respectively.

All in all, dPG-norbonene is the most promising candidate for nanogel formation with dPG-metTet, within the series of dienophile macromonomers presented in this work, in terms of synthetic access to the precursors, scalability, and reproducibility of the system. Thus, the goal for future studies will be the preparation of responsive nanogels based on dPG-norbonene/dPG-metTet for the triggered degradation and release of therapeutic proteins.

Experimental Section

Materials: The solvents *n*-pentane, ethyl acetate, and diethyl ether were obtained from the technically pure solvents by distillation before use. DCM and acetone (HPLC grade) were used without further purification. Dry DCM and THF were taken from a SPS-800 type MBRAUN solvent drying system. Dry methanol and DMF were acquired from Acros and Fischer Chemical. All other chemicals and deuterated solvents were purchased from Sigma Aldrich, Merck, Acros, and Fisher Chemicals and were used as reagent grade without further purification. Qualitative thin layer chromatography (TLC) was performed on silica gel-coated aluminum plates serving as stationary phase (silica gel 60 F254 from Macherey-Nagel). The analytes were identified by irradiation of the TLC plates with UV light ($\lambda = 254$ nm) or by treatment with a potassium-permanganate-based staining reagent (100 mL deionized water, 200 mg potassium permanganate) or anis aldehyde-based (450 mL EtOH, 25.0 mL anis aldehyde, 25.0 mL conc. sulfuric acid, 8.0 mL acetic acid). Column chromatography was performed with silica gel of the company Macherey-Nagel (grain size 40–63 µm, 230–400 mesh) as stationary phase and the indicated eluent mixtures as mobile phase.

Analytical Methods: IR spectra were recorded on a JASCO FT/IR-4100 spectrometer. The characteristic absorption bands were given in wave numbers. ^{1}H NMR spectra were recorded at 300 K on Joel ECX 400 (400 MHz) and AVANCE III (700 MHz) instruments. Chemical shifts δ were indicated in parts per million (ppm) relative to tetramethyl silane (0 ppm) and calibrated as an internal standard to the signal of the incompletely deuterated solvent ($CDCl_3$: $\delta = 7.26$ ppm, MeOD: $\delta = 3.31$ ppm). Coupling constants J were given in Hertz. ^{13}C NMR spectra were recorded at 300 K on AVANCE III instruments (176 MHz). Chemical shifts δ were given in ppm relative to tetramethyl silane (0 ppm) and calibrated as an internal standard to the signal of the incompletely deuterated solvent ($CDCl_3$: $\delta = 77.16$ ppm, MeOD: $\delta = 49$ ppm). Coupling constants J were given in Hertz. The spectra were decoupled from proton broadband. DLS and Zeta potential were measured on a Malvern zeta-sizer nano ZS 90 with He–Ne laser ($\lambda = 532$ nm) at 173° backscatter and automated attenuation at 25 °C. Three measurements were performed per sample with between 10 and 16 individual measurements, yielding a mean size value plus standard deviation. Sample concentration was kept at 1 mg mL^{-1}. GPC was performed on an Agilent 1100 at 5 mg mL^{-1} using a pullulan standard, 0.1 M NaNO3 solution as eluent, and a PSS Suprema column 10 µm with a flow rate of 1 mL min^{-1}. Signals were detected with an RI detector.

Precursors and Macromonomers: All air- and moisture-sensitive reactions were carried out in flasks in an inert atmosphere (argon) using conventional Schlenk techniques. Reagents and solvents were added via argon rinsed disposable syringes. Solids were added in argon counterflow or in solution.

The synthesis of the literature known precursors is described in the Supporting Information, showing the modified procedures.

Bicyclo[2.2.1]hept-5-en-2-ylmethyl (4-nitrophenyl) Carbonate (1): In a dried 500 mL Schlenk flask, bicyclo[2.2.1]hept-5-en-2-ylmethanol (2.5 g, 20 mmol) and pyridine (4 mL, 50 mmol) were dissolved in dry DCM (235 mL) under an argon atmosphere and stirred for 5 min. Then, 4-nitrophenyl chloroformate (6 g, 30 mmol) was added and the reaction was stirred at room temperature for 90 min. After quenching with 200 mL of saturated ammonium chloride solution, the water phase was extracted three times with 100 mL DCM each. The organic phases were united and dried over sodium sulfate and the solvent was removed under reduced pressure. The raw product was purified with column chromatography using silica and pentane:EtOAc as solvent system (10:1; $R_f = 0.6$ in pentane:EtOAc 10:1). The product was obtained as a colorless solid and stored in the freezer (5.5 g, 87%). ^{1}H NMR (700 MHz, CD_3OD): δ 8.27 (m, 2 H, aryl), 7.43–7.34 (m, 2 H), 6.22–5.98 (m, 2 H, $R^1HC = CHR^2$), 4.36–3.86 (m, 2 H, RCH_2OCO_2R), 2.96–2.80 (m, 2 H, bridgehead-H), 2.57–2.46 (m, 1 H, $R^3R^4CHCH_2OR^5$), 1.94–0.58 (m, 4 H, bridge-H atoms + $R^6CH_2CR^7CH_2OR^5$). ^{13}C NMR (176 MHz, CD_3OD): δ 157.3, 154.1, 146.9, 139.0, 138.2, 137.3, 133.1, 126.3, 123.4, 74.4, 73.8, 50.5, 45.9, 45.2, 44.9, 43.6, 42.9, 39.4, 39.1, 30.4, 29.8.

General Procedure for dPG-Dienophiles: All dPG-dienophiles were synthesized according to the same general procedure. As an example, dPG–norbonene is described in detail.

dPG-Norbonene$_{9\%}$ (MM2): In a 50 mL Schlenk flask, dry DMF (15 mL) was added to a methanolic solution of dPG-amine (22.22 mL, 0.09 g mL^{-1}). Methanol was removed under reduced pressure, fresh dry DMF (15 mL) was added, the solution was constricted under reduced pressure to 25 mL and Et_3N (0.82 g, 8.11 mmol, 1.12 mL) was added. Bicyclo[2.2.1]hept-5-en-2-ylmethyl (4-nitrophenyl) carbonate (0.94 g, 2.97 mmol) (or other activated carbonate of dienophile) was dissolved in DMF (10 mL) and the solution was added dropwise via syringe to the dPG-amine solution. The resulting reaction mixture was stirred at room temperature overnight. The crude product was dialyzed against a mixture of water and acetone (1:1) for 3 days and methanol for 2 days (MWCO = 1 kDa). The product was obtained as a slightly yellow methanolic solution (9% functionalization, 83%). ^{1}H NMR (700 MHz, CD_3OD, δ): 6.25–6.21 (m, 1 H, H-olefin), 6.05–6.00 (m, 1 H, H-olefin), 3.98–3.48 (dPG-backbone), 2.98–2.92 (m, 1 H, H-bridgehead), 2.89–2.84 (m, 1 H, H-bridgehead), 2.49–2.42 (m, 1 H, H-bridgehead), 1.94–1.88 (m, 1 H, H-bridge), 1.51–1.47 (m, 1 H, H-bridge), 1.37–1.32 (m, 1 H, H-bridge), 0.64–0.59 (m, 1 H, H-ring). ^{13}C NMR (176 MHz, CD_3OD, δ): 159.3, 138.6, 138.0, 137.4, 133.3, 81.4, 79.9, 74.0, 72.6, 72.4, 72.24, 70.7, 69.4, 64.4, 62.8, 50.4, 49.9, 45.1, 44.9, 43.5, 42.8, 39.8, 39.5, 30.5, 29.9. IR (ATR): $\tilde{\nu}$ = 3364, 2910, 2871, 1697, 1540, 1418, 1457, 1418, 1327, 1254, 1107, 1076 cm^{-1}.

dPG-BCN$_{7.5\%}$ (MM1): dPG-BCN was synthesized according to a literature protocol. dPG-amine (22.22 mL, 0.09 g mL^{-1}); Et_3N (0.82 g, 8.11 mmol, 1.12 mL); BCN (0.94 g, 2.97 mmol). The product was obtained as a yellow methanolic solution (7.5% functionalization, 85%). ^{1}H NMR (700 MHz, CD_3OD, δ): 4.22–3.35 (dPG-backbone), 2.47–2.12 (m, 4 H, H-vinyl), 1.72–1.32 (m, 4 H, H-ring), 1.04–0.93 (m, 1 H, H-cyclopropane), 0.85–0.71 (m, 2 H, H-cyclopropane). ^{13}C NMR (176 MHz, CD_3OD, δ): 99.7, 81.5, 80.0, 74.0, 73.1, 72.6, 72.3, 72.3, 71.0, 70.7, 64.5, 64.4, 63.0, 34.5, 30.3, 25.1, 24.2, 22.1, 21.4. IR (ATR): $\tilde{\nu}$ = 3379, 2915, 2873, 1696, 1614 1517, 1457, 1394, 1304, 1244, 1078, 934 cm^{-1}.

dPG-Cyclopropene$_{8\%}$ (MM3): dPG-amine (5.55 mL, 0.09 g mL^{-1}); Et_3N (0.21 g, 2.03 mmol, 0.28 mL); (2-methylcycloprop-2-en-1-yl)methyl 2-(4-nitrophenyl)acetate (0.22 g, 0.88 mmol). The product was obtained as a colorless methanolic solution (8% functionalization, 85%). ^{1}H NMR (700 MHz, CD_3OD, δ): 6.76–6.69 (m, 1 H, H-olefin), 3.97–3.46 (m, dPG-backbone), 2.25–2.15 (m, 3 H, methyl), 1.73–1.63 (m, 1 H, H-ring). ^{13}C NMR (176 MHz, CD_3OD, δ): 122.2, 103.1, 81.5, 79.9, 74.0, 73.4, 72.5, 72.2, 70.9, 70.7, 64.5, 64.4, 62.8, 18.4, 11.8. IR (ATR): $\tilde{\nu}$ = 3374, 2912, 2876, 1697, 1541, 1457, 1325, 1259, 1110, 1080, 874, 848 cm^{-1}. EA ($C_{72}H_{136}N_2O_{43}$): calc. C (50.34%), found C (50.36%); calc. N (1.63%), found N (2.45%); calc. H (7.98%), found (7.96%).

dPG-DHP$_{9\%}$ (MM4): dPG-amine (5.55 mL, 0.09 g mL^{-1}); Et_3N (0.15 g, 1.52 mmol, 0.21 mL); (3,4-dihydro-2H-pyran-2-yl)methyl (4-nitrophenyl) carbonate (0.16 g, 0.56 mmol). The product was obtained as a colorless methanolic solution (9% functionalization, 82%). ^{1}H NMR (700 MHz, CD_3OD, δ): 6.41–6.34 (m, 1 H, $R^1HC = CHOR^2$), 4.78–4.72 (m, 1 H, $R^3OHC = CHR^1$), 4.22–4.13 (m, 2 H, $R^4OCHR^5R^6$), 4.07–3.44 (dPG-backbone), 2.19–1.96 (m, 2 H, H-ring), 1.96–1.67 (m, 2 H, H-ring). ^{13}C NMR (176 MHz, CD_3OD, δ): 101.8, 101.7, 81.7, 81.5, 79.9, 74.5, 74.0, 73.0, 72.5, 72.3, 71.0, 71.0, 70.7, 67.8, 64.5, 64.4, 62.7, 49.9, 25.3, 20.2. IR (ATR): $\tilde{\nu}$ = 3384, 2913, 2874, 1701, 1650, 1541, 1457, 1418, 1329, 1240, 1111, 1070 cm^{-1}. EA ($C_{726}H_{1366}N_{20}O_{435}$): calc. C (50.30%), found C (48.86%); calc. N (1.62%), found (2.18%); calc. H (7.94%), found H (8.47%).

dPG-metTet$_{6.5\%}$ (MM5): In a 250 mL Schlenk flask, dry DMF (50 mL) was added to a methanolic solution of dPG-amine (44.44 mL, 0.09 g mL^{-1}). Methanol was removed under reduced pressure, fresh dry DMF (50 mL) was added, and the solution was constricted under reduced pressure to 75 mL. The 4-(6-methyl-1,2,4,5-tetrazin-3-yl)benzoic acid (0.89 g, 4.05 mmol), EDC·HCl (1.04 g, 5.41 mmol), HOBT (0.73 g, 5.41 mmol), and DIPEA (1.05 g, 5.41 mmol, 1.38 mL) were dissolved in dry DMF (50 mL) and the solution was added dropwise via syringe to the

dPG-amine solution. The resulting reaction mixture was stirred at room temperature overnight. The crude product was dialyzed against DMF for 4 days and methanol for 4 days (MWCO = 1 kDa). The product was obtained as a red methanolic solution (6.5% functionalization, 85%). ^{1}H NMR (700 MHz, CD_3OD, δ): 8.69–8.53 (m, 2 H, H-aryl), 8.12–7.98 (m, 2 H, H-aryl), 4.05–3.48 (m, dPG-backbone), 3.10 (s, 3 H, methyl-H).^{13}C NMR (CD_3OD, 176 MHz, δ): 169.4, 169.2, 164.8, 139.1, 136.3, 129.4, 128.9, 81.7, 81.4, 80.2, 79.8, 74.0, 73.0, 72.5, 72.2, 71.0, 70.7, 70.3, 64.5, 64.4, 62.8. IR (ATR): $\tilde{\nu}$ = 3348, 2871, 1644, 1548, 1456, 1404, 1364, 1327, 1305, 1258, 1070, 931 cm^{-1}.

Macrogel Formation: The time required for the gelation of a mixture of dPG-metTet with the respective dPG-dienophile was measured. For each experiment, 50 µL of macromonomer solution was used (20 µL of dPG-metTet + 30 µL of dPG-dienophile) at a concentration of 200 mg mL^{-1}. The mixture was added to a small glass vial and after defined time spans, the vial was tilted at an angle of 45° to see if the mixture started to gelate. This was confirmed by the inability of the gels to flow down the glass vial. For samples that did not gelate even after 30 min, the time it took for the macromonomer mixture to flow from the top of the vial to the bottom of the vial was measured and compared to just dPG-metTet solution.

Nanogel Formation: General Procedure—The ratios of macromonomer A (dPG-metTet) to macromonomer B (dPG-dienophile) were set to 1:1.5. Acetone was utilized as the non-solvent. Parameters such as solvent to non-solvent ratio (1:10–1:200), macromonomer concentration in water (0.5–7.5 mg mL^{-1}), stirring speed (300–1200 rpm), chemical quenching time $T_{q,chem}$ (0–∞ min), and water quenching time $T_{q,water}$ (0–120 min) were varied. As an example, a general procedure for one set of parameters is described below.

Macromonomers A and B were stored as stock-solutions in water. An aliquot was taken and separately diluted with water to a final volume of 1 mL. For this, 15 µL of macromonomer A were diluted with 485 µL water and 22.5 µL of macromonomer B with 477.5 µL water. Both solutions were cooled in an ice bath to 4 °C. Macromonomer A solution was added fast to solution B and shortly vortexed for 5 s. Then, the mixed solution was added very fast via syringe to a glass vial containing magnetically stirred acetone (40 mL) at 1200 rpm. The turbid dispersion was stirred for another 2 s and then kept still for 10 min. The reaction was then quenched by the addition of 20 µL of 2-(vinyloxy)ethan-1-ol. Water (1/3 of acetone) was added after 30 min and the acetone was removed under reduced pressure. Purification was performed by centrifugal filtration, using a membrane with a cutoff of 300 kDa and three consecutive washing steps with 10 mL each. Nanogels were obtained as stable dispersions in water and characterized using DLS, NTA, and Zeta-potential measurements.

Coprecipitation of Myoglobin: The inverse nanoprecipitation was performed as described in the general procedure for nanogel formation. Varying amounts of a stock solution of myoglobin were added to the dPG-metTet macromonomer solution and thoroughly mixed. The total volume of water was kept at 1 mL. 2.5 and 5 wt% of myoglobin were encapsulated each for dPG-norbonene- and dPG-cyclopropene-NGs (n = 3). The gels were purified by centrifugation filtration, using filters with a molecular weight cutoff of 1 MDa at 234 rcf. The gel volume was reduced to 1 mL and fresh PBS buffer solution was added (10 mL). Then, the volume was reduced to 1 mL again and the whole process was repeated three times to ensure the complete removal of the nonencapsulated protein.

Protein Content Determination Assay: A standard Pierce BCA assay kit was used for the determination of protein content within the nanogels. 25 µL of the purified nanogels were added to a 96-well plate. Then, 200 µL of working reagent was added to each well and the plate was shaken for 30 s on a plate shaker. The plate was then incubated at 37 °C for 1 h. After cooling to room temperature, the absorbance was measured at 562 nm on a plate reader. Samples were recorded in triplicates and for three independent gels of the same type. Calibration curves were prepared for a dilution series of albumin and myoglobin in the range of 0–750 µg mL^{-1}. Concentrations of myoglobin in the samples were determined via the fitted standard curves of myoglobin (Figure S6, Supporting Information).

Supporting Information

Supporting Information is available from the Wiley Online Library or from the author.

Acknowledgements

The authors like to acknowledge Cathleen Schlesener for providing dPG and dPG-NH_2 and the BioSupraMol core facility for NMR and ESI measurements. Dr. Pamela Winchester is thanked for careful proofreading this manuscript. SFB 765 is thanked for funding.

Conflict of Interest

The authors declare no conflict of interest.

Keywords

inverse electron demand Diels Alder, nanogels, nanoprecipitation, protein encapsulation

Received: September 24, 2019
Revised: October 25, 2019
Published online: November 21, 2019

[1] H. S. Choi, W. Liu, P. Misra, E. Tanaka, J. P. Zimmer, B. Itty Ipe, M. G. Bawendi, J. V Frangioni, *Nat. Biotechnol.* **2007**, *25*, 1165.
[2] L. W. Seymour, R. Duncan, J. Strohalm, J. Kopeček, *J. Biomed. Mater. Res.* **1987**, *21*, 1341.
[3] P. Zhang, F. Sun, S. Liu, S. Jiang, *J. Controlled Release* **2016**, *244*, 184.
[4] P. L. Turecek, M. J. Bossard, F. Schoetens, I. A. Ivens, *J. Pharm. Sci.* **2016**, *105*, 460.
[5] R. Haag, F. Kratz, *Angew. Chem., Int. Ed.* **2006**, *45*, 1198.
[6] K. Knop, R. Hoogenboom, D. Fischer, U. S. Schubert, *Angew. Chem., Int. Ed.* **2010**, *49*, 6288.
[7] D. Steinhilber, M. Witting, X. Zhang, M. Staegemann, F. Paulus, W. Friess, S. Küchler, R. Haag, *J. Controlled Release* **2013**, *169*, 289.
[8] S. Singh, F. Topuz, K. Hahn, K. Albrecht, J. Groll, *Angew. Chem., Int. Ed.* **2013**, *52*, 3000.
[9] C. Wu, C. Böttcher, R. Haag, *Soft Matter* **2015**, *11*, 972.
[10] T. Nochi, Y. Yuki, H. Takahashi, S. Sawada, M. Mejima, T. Kohda, N. Harada, I. G. Kong, A. Sato, N. Kataoka, D. Tokuhara, S. Kurokawa, Y. Takahashi, H. Tsukada, S. Kozaki, K. Akiyoshi, H. Kiyono, *Nat. Mater.* **2010**, *9*, 572.
[11] D. Steinhilber, S. Seiffert, J. A. Heyman, F. Paulus, D. A. Weitz, R. Haag, *Biomaterials* **2011**, *32*, 1311.
[12] E. Mauri, G. Perale, F. Rossi, *ACS Appl. Nano Mater.* **2018**, *1*, 6525.
[13] D. Steinhilber, A. L. Sisson, D. Mangoldt, P. Welker, K. Licha, R. Haag, *Adv. Funct. Mater.* **2010**, *20*, 4133.
[14] A. V. Kabanov, S. V. Vinogradov, *Angew. Chem., Int. Ed.* **2009**, *48*, 5418.
[15] H. Zhou, D. Steinhilber, H. Schlaad, A. L. Sisson, R. Haag, *React. Funct. Polym.* **2011**, *71*, 356.
[16] D. Klinger, K. Landfester, *J. Polym. Sci., Part A: Polym. Chem.* **2012**, *50*, 1062.
[17] A. L. Sisson, D. Steinhilber, T. Rossow, P. Welker, K. Licha, R. Haag, *Angew. Chem., Int. Ed.* **2009**, *48*, 7540.
[18] A. L. Sisson, I. Papp, K. Landfester, R. Haag, *Macromolecules* **2009**, *42*, 556.

[19] D. Steinhilber, S. Seiffert, J. A. Heyman, F. Paulus, D. A. Weitz, R. Haag, *Biomaterials* **2011**, *32*, 1311.
[20] M. Antonietti, *Angew. Chem. Int. Ed.* **1988**, *27*, 1743.
[21] J. Z. Du, T. M. Sun, W. J. Song, J. Wu, J. Wang, *Angew. Chem., Int. Ed.* **2010**, *49*, 3621.
[22] K. McAllister, P. Sazani, M. Adam, M. J. Cho, M. Rubinstein, R. J. Samulski, J. M. DeSimone, *J. Am. Chem. Soc.* **2002**, *124*, 15198.
[23] R. Jenjob, T. Phakkeeree, F. Seidi, M. Theerasilp, D. Crespy, *Macromol. Biosci.* **2019**, *19*, e1900063.
[24] R. L. Grant, C. Yao, D. Gabaldon, D. Acosta, *Toxicology* **1992**, *76*, 153.
[25] Â. S. Inácio, K. A. Mesquita, M. Baptista, J. Ramalho-Santos, W. L. C. Vaz, O. V. Vieira, *PLoS One* **2011**, *6*, e19850.
[26] S. Schubert, J. T. Delaney, U. S. Schubert, *Soft Matter* **2011**, *7*, 1581.
[27] C. Zhang, V. J. Pansare, R. K. Prud'homme, R. D. Priestley, *Soft Matter* **2012**, *8*, 86.
[28] R. Tong, L. Yala, T. M. Fan, J. Cheng, *Biomaterials* **2010**, *31*, 3043.
[29] Y. Dai, X. Chen, X. Zhang, *Macromol. Rapid Commun.* **2019**, *40*, 1.
[30] D. C. Kennedy, C. S. McKay, M. C. B. Legault, D. C. Danielson, J. A. Blake, A. F. Pegoraro, A. Stolow, Z. Mester, J. P. Pezacki, *J. Am. Chem. Soc.* **2011**, *133*, 17993.
[31] N. J. Agard, J. a. Prescher, C. R. Bertozzi, *J. Am. Chem. Soc.* **2004**, *126*, 15046.
[32] D. P. Nair, M. Podgórski, S. Chatani, T. Gong, W. Xi, C. R. Fenoli, C. N. Bowman, *Chem. Mater.* **2014**, *26*, 724.
[33] A. L. Sisson, R. Haag, *Soft Matter* **2010**, *6*, 4968.
[34] J. Khandare, M. Calderón, N. M. Dagia, R. Haag, *Chem. Soc. Rev.* **2012**, *41*, 2824.
[35] M. Dimde, D. Steinhilber, F. Neumann, Y. Li, F. Paulus, N. Ma, R. Haag, *Macromol. Biosci.* **2016**, *17*, 1600190.
[36] M. Dimde, F. Neumann, F. Reisbeck, S. Ehrmann, J. L. Cuellar-Camacho, D. Steinhilber, N. Ma, R. Haag, *Biomater. Sci.* **2017**, *5*, 2328.
[37] P. Dey, T. Bergmann, J. L. Cuellar-Camacho, S. Ehrmann, M. S. Chowdhury, M. Zhang, I. Dahmani, R. Haag, W. Azab, *ACS Nano* **2018**, *12*, 6429.
[38] R. A. Carboni, R. V. Lindsey, *J. Am. Chem. Soc.* **1959**, *81*, 4342.
[39] J. Sauer, D. K. Heldmann, J. Hetzenegger, J. Krauthan, H. Sichert, J. Schuster, *Eur. J. Org. Chem.* **1998**, *1998*, 2885.
[40] G. Clavier, P. Audebert, *Chem. Rev.* **2010**, *110*, 3299.
[41] B. L. Oliveira, Z. Guo, G. J. L. Bernardes, *Chem. Soc. Rev.* **2017**, *46*, 4895.
[42] D. S. Liu, A. Tangpeerachaikul, R. Selvaraj, M. T. Taylor, J. M. Fox, A. Y. Ting, *J. Am. Chem. Soc.* **2012**, *134*, 792.
[43] J. Schoch, M. Staudt, A. Samanta, M. Wiessler, A. Jäschke, *Bioconjugate Chem.* **2012**, *23*, 1382.
[44] J. Yang, J. Šečkute, C. M. Cole, N. K. Devaraj, *Angew. Chem., Int. Ed.* **2012**, *51*, 7476.
[45] M. Witting, M. Molina, K. Obst, R. Plank, K. M. Eckl, H. C. Hennies, M. Calderón, W. Frieß, S. Hedtrich, *Nanomed.: Nanotechnol., Biol. Med.* **2015**, *11*, 1179.
[46] M. R. Karver, R. Weissleder, S. A. Hilderbrand, *Bioconjugate Chem.* **2011**, *22*, 2263.
[47] D. Ekinci, A. L. Sisson, A. Lendlein, *J. Mater. Chem.* **2012**, *22*, 21100.
[48] C. Siegers, M. Biesalski, R. Haag, *Chem. - Eur. J.* **2004**, *10*, 2831.
[49] K. Lang, L. Davis, S. Wallace, M. Mahesh, D. J. Cox, M. L. Blackman, J. M. Fox, J. W. Chin, *J. Am. Chem. Soc.* **2012**, *134*, 10317.
[50] N. K. Devaraj, R. Weissleder, S. A Hilderbrand, *Communications* **2008**, *19*, 2297.
[51] F. Thalhammer, U. Wallfahrer, J. Sauer, *Tetrahedron Lett.* **1990**, *31*, 6851.
[52] B. D. Chithrani, A. A. Ghazani, W. C. W. Chan, *Nano Lett.* **2006**, *6*, 662.
[53] S. Mitragotri, J. Lahann, *Nat. Mater.* **2009**, *8*, 15.
[54] D. M. Patterson, L. A. Nazarova, B. Xie, D. N. Kamber, J. A. Prescher, *J. Am. Chem. Soc.* **2012**, *134*, 18638.